Experimental and Theoretical Study of Hyperconjugative Interaction Effects on NMR $^1J_{CH}$ Scalar Couplings

Rubén H. Contreras,[†] Ángel L. Esteban,[‡] Ernesto Díez,[§] Ernest W. Della,[||] Ian J. Lochert,[||,⊥] Francisco P. dos Santos,[#] and Cláudio F. Tormena*[,#]

Departamento de Física, FCEyN, Universidad de Buenos Aires, Ciudad Universitaria, P. 1 and CONICET (C1428EHA) Buenos Aires, Argentina, Departamento de Química Física, Universidad de Alicante, Apartado 99, E-03080 Alicante, Spain, Departamento de Química Física Aplicada, Facultad de Ciencias, C2, Universidad Autónoma de Madrid, E-28049 Madrid, Spain, Department of Chemistry, Flinders University, Bedford Park, South Australia 5108, Australia, and Departamento de Química, Faculdade de Filosofia Ciências e Letras de Ribeirão Preto, Universidade de São Paulo, Avenue Bandeirantes 3900, 14040-901, Ribeirão Preto, Sao Paulo, Brazil

Received: September 28, 2005; In Final Form: December 6, 2005

Hyperconjugative and electrostatic interactions effects on $^1J_{CH}$ spin−spin coupling constants (SSCCs) are critically studied from both theoretical and experimental points of view. A qualitative model is used to predict how the former affect such SSCCs, while electrostatic interactions are modeled with a point charge placed in the vicinity of the corresponding σ_{CH} bond. Hyperconjugative interactions are calculated using the "natural bond orbital" approach, and using the point-charge model, it is shown how intertwined are both types of interactions. Several members of the series 1-X-bicyclo[1.1.1]pentane and 1-X-3-methylbicyclo[1.1.1]pentane are chosen as model compounds for measuring $^1J_{CH}$ SSCCs; in some of them were performed also DFT-SSCC calculations. The strained cage substrate in these series defines strong σ-hyperconjugative interactions, making these compounds excellent examples to verify the qualitative model presented in this work. It is verified that (a) hyperconjugative interactions from the σ_{CH} bond or into the σ^*_{CH} antibond containing the coupling nuclei yield a decrease of the corresponding $^1J_{CH}$ SSCC and (b) hyperconjugative interactions from other bonds involving the coupling C nucleus yield an increase of that $^1J_{CH}$ SSCC.

1. Introduction

The importance of hyperconjugative interactions in modern organic chemistry is nowadays well-recognized, and in the current bibliography extensive lists of recent works can be found.[1] Qualitative descriptions of several aspects of such interactions can be obtained resorting to the simple PMO theory.[2] Quantitative descriptions of hyperconjugative interactions can be obtained employing Weinhold's Natural Bond Orbitals (NBO) method.[3] Interactions of types $n \rightarrow \sigma^*$, $\sigma \rightarrow \pi^*$, $\pi \rightarrow \sigma^*$, and $\sigma \rightarrow \sigma^*$ can affect spin−spin coupling constants (SSCCs) significantly;[4] therefore, if properly understood the way in which they are affected, SSCCs can be used as probes to study hyperconjugative interactions.[5] The first type is part of the "anomeric effect"[6] and is known as "negative hyperconjugative interaction";[7] generally, it is notably stronger than the latter three. The second and third types are accepted to be the main transmission mechanism for the Fermi contact (FC) term of long-range benzylic-like couplings.[8] The fourth type is now known to transmit the FC term of long-range SSCCs in strained saturated compounds.[9]

The influence of negative hyperconjugative effects on $^1J_{CH}$ SSCCs has been discussed extensively by several authors;[10] and the closely related lone-pair orientation effect on SSCCs was also discussed.[11] However, in a recent paper Cuevas et al.[12] expressed "... the $^1J_{CH}$ value in HCOC fragments is definitely not a consequence of $n(O) \rightarrow \sigma^*_{CH}$ delocalization, despite expectations, although a small contribution cannot be excluded." In that paper, Cuevas et al. concluded that the main contribution to the Perlin effect[13] comes from a polarization effect. In several papers the influence of proximate electrostatic effects on $^1J_{CH}$ was studied from different points of view, like for instance, in "improper" hydrogen bonds or considering an electric field along the corresponding σ_{CH} bond.[14] Nowadays, it is well-known that hyperconjugative interactions involving either a σ_{CH} bond or its corresponding antibond can be inhibited (enhanced) depending on the orientation of an electric field along that bond.[5c] Therefore, a careful study of hyperconjugative effects on $^1J_{CH}$ SSCCs cannot neglect how intertwined are these interactions with electrostatic effects.

In this paper an experimental and theoretical study is carried out in order to obtain a better understanding of how delocalization interactions affect $^1J_{CH}$ SSCCs. It is already well-known that for a σ_{CH} bond α to a π-electronic system, like those of the methyl group in toluene, interactions of type $\sigma_{CH} \rightarrow \pi^*$ and $\pi \rightarrow \sigma^*_{CH}$ yield a reduction in the corresponding $^1J_{CH}$ SSCC.[5a,c] In Section 2, a qualitative theoretical analysis is applied to predict the influence of different hyperconjugative interactions on $^1J_{CH}$ SSCCs. From such an approach a few simple rules are established, although it is important to recall that they are

* Corresponding author. E-mail: tormena@ffclrp.usp.br. Fax: +55-16-3633-8151. Phone: +55-16-3602-4382.
[†] Universidad de Buenos Aires and CONICET.
[‡] Universidad de Alicante.
[§] Universidad Autónoma de Madrid.
[||] Flinders University.
[⊥] Present address: Defense Science and Technology Organization, Weapons Systems Division, P.O. Box 1500, Salisbury, South Australia 5108, Australia.
[#] Universidade de São Paulo.

10.1021/jp0555201 CCC: $33.50
Published on Web 03/03/2006

obtained only on a qualitative base. In Section 3, experimental as well as computational details are provided. Since it is known that electrostatic effects may affect some hyperconjugative interactions as well as some $^1J_{CH}$ SSCCs, in a subsequent section they are studied resorting to three different model systems in which very different hyperconjugative interactions take place.

Looking for molecular systems where experimental evidence supporting the simple rules obtained in Section 2, it was thought that compounds of these two series 1-X-bicyclo[1.1.1]pentane (**Ia**) and 1-X-3-methylbicyclo[1.1.1]pentanes (**Ib**) could well be adequate model systems. The main reasons to make this choice are as follows. In these strained cyclic compounds delocalization interactions are notably enhanced;[15] such interactions should be notably affected by some substituents. The orientation of the σ_{CH} bond whose $^1J_{CH}$ SSCC will be used as a probe to verify such rules is adequate to isolate at least some of the expected effects. In this way, 24 members of series **Ia** and 16 members of series **Ib** were chosen to perform the present study; in compounds of the **Ia** series very small $^{13}C_1-$SCS were reported,[16] and such a behavior was rationalized as originating mainly in the very strong $\sigma_{C_2C_3} \rightarrow \sigma^*_{C_1X_\alpha}$ hyperconjugative interactions (and their analogs involving the other two bridge carbon atoms). In **Ib** the similar $^{13}C_1-$SCS are slightly increased[17] in comparison with those of **Ia**. It is also known that in series **Ia** unusual substituent effects on $^3J_{C_1H}$ SSCCs were observed,[18] and they were correlated with the strong changes on delocalization interactions induced by an X substituent.[19] These considerations suggest that $^1J_{C_3H}$ SSCCs in series **Ia** should also depend rather strongly on the X substituent. The "lateral" $^1J_{C_2H}$ SSCCs in series **Ia** and **Ib** are expected to show substituent effects that might be rationalized in terms of differences in electron delocalization interactions. Such $^1J_{CH}$ SSCCs were measured, and for a choice of substituents, they were also calculated using the CP-DFT methodology[20] as implemented in the Gaussian 03 package of programs.[21] Hyperconjugative interactions were evaluated using the NBO method as implemented[22] in that suite of programs.

2. Theoretical Predictions about Hyperconjugative Effects on $^1J_{CH}$ SSCCs

According to the nonrelativistic Ramsey's formulation, isotropic SSCCs are contributed by four terms, namely, Fermi contact (FC), spin−dipolar (SD), paramagnetic spin−orbit (PSO), and diamagnetic spin−orbit (DSO) as shown in eq 1:

$$^1J_{CH} = {}^{FC}J_{CH} + {}^{SD}J_{CH} + {}^{PSO}J_{CH} + {}^{DSO}J_{CH} \qquad (1)$$

Each of these terms can be decomposed into localized molecular orbital (LMO) contributions. Within the polarization propagator approach,[23] the three second-order terms can be expressed as shown in eq 2:

$$^1J_{CH} = \sum_{ia,jb} {}^1J_{ia,jb}(CH) \qquad (2)$$

where i and j are occupied LMOs, while a and b are vacant LMOs. For $^1J_{CH}$ SSCCs, it is known that the FC term is by far the most important one. Therefore, for this qualitative analysis aimed at obtaining insight into how different hyperconjugative interactions affect $^1J_{CH}$ SSCCs, it is enough to consider the FC term. As shown previously,[23b−d] the LMO contributions to the FC term can be written as in eq 3:

$$^1J^{FC}_{ia,jb}(CH) = W_{ia,jb}[U_{ia,C}U_{jb,H} + U_{ia,H}U_{jb,C}] \qquad (3)$$

where $U_{ia,C}(U_{jb,H})$ are the "perturbators" (i.e., the matrix elements of the FC operator between the occupied i (j) and vacant a (b) LMOs evaluated at the C (H) site of the coupling nuclei), and they give a measure of the strength of the $i \rightarrow a$ ($j \rightarrow b$) virtual excitation due to that operator. $W_{ia,jb}$ are the polarization propagator matrix elements, and they correspond to the response of the electronic molecular system to the presence of the electron−nucleus FC interaction, connecting two virtual excitations $i \rightarrow a$ and $j \rightarrow b$. These matrix elements decrease when increasing the $\epsilon_{i\rightarrow a}$ and $\epsilon_{j\rightarrow b}$ energy gaps between these occupied and vacant LMOs involved in each virtual excitation.

In the particular case of the FC term of $^1J_{CH}$ SSCCs, the sum in eq 2 is largely dominated by the following two types of terms:

(1) $i = j$ corresponds to the LMO localized on the σ_{CH} bond involving the coupling nuclei, and $a = b$ corresponds to the vacant LMO localized at that σ_{CH} bond. The corresponding term in eq 2 is dubbed the "bond contribution" (J^b).

(2) Either i or j corresponds to the LMO on the σ_{CH} bond containing the coupling nuclei, and j or i corresponds to an occupied LMO on other σ_{CX} bond involving the C coupling nucleus; and $a = b$ correspond to localized vacant MOs placed at that σ_{CH} bond containing the coupling nuclei. The corresponding term in eq 2 is dubbed "other bond contribution" (J^{ob}). However, it should be stressed that this term involves also the σ_{CH} bond and antibond containing the coupling nuclei.

For $^1J_{CH}$ SSCCs, the J^b contribution is positive while the J^{ob} one is negative, having the former a notable larger absolute value than the latter. Since only a qualitative description is sought here, occupied and vacant LMOs in eq 2 can be taken approximately as bond and antibonding orbitals of the NBO description. Using this choice, it will be easy to identify how hyperconjugative interactions affect the J^b and J^{ob} contributions. With this idea in mind, the polarization propagator matrix elements in eq 3 decrease whenever there is an interaction increasing the energy gap between the i or j and the a or b antibonding NBOs.

Interactions that increase the relevant energy gaps in J^b are (1) hyperconjugative interactions into the antibonding orbital (σ^*_{CH}) where the σ_{CH} bond contains the coupling nuclei; (2) hyperconjugative interactions from the σ_{CH} bond containing the coupling nuclei. Interactions that increase the relevant energy gaps in J^{ob} are (3) hyperconjugative interactions from the bonding orbital that correspond to "other bond" (i.e., bonds involving the C coupling nucleus, but otherwise they are other than that containing the coupling proton). (4) The same as those quoted above for the J^b contribution (i.e., 1 and 2). However, since the absolute values of J^{ob} are notable smaller than that of J^b, this effect, from a qualitative point of view, can be neglected.

Factors affecting the "perturbators" ($U_{ia,C}$ and $U_{jb,C}$) are the s % character of the LMO orbitals i, j and a, b at the C atom, for example, these contributions are larger when the s % character is larger (it is assumed that changes in the s % character at the H site are much less important than those at the C atom).

The above considerations on the energy gap between an occupied, i, and a vacant, a, LMO can be interpreted resorting to the simple PMO theory (Figure 1). In fact, this shows schematically why a hyperconjugative interaction from the σ_{CH} bond, $\sigma_{CH} \rightarrow \sigma^*_{BD}$, yields a decrease of J^b corresponding $^1J_{CH}$ SSCC (σ^*_{BD} stands for any antibonding orbital belonging to the compound under study). It should be noted that this effect also appears in J^{ob} but, since the absolute value of J^b is notably larger than that of J^{ob}, in a qualitative analysis it can be expected

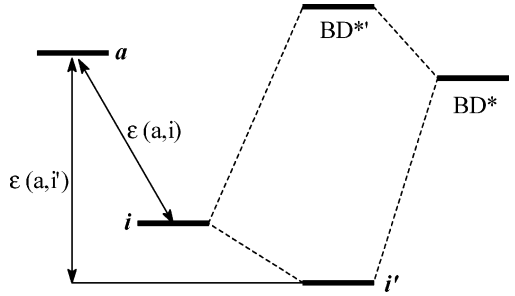

Figure 1. If the occupied ***i*** orbital undergoes a hyperconjugative interaction of type ***i*** → **BD***, then according to the simple PMO theory, the energy gap between these two orbitals change from ϵ**(a**, ***i*****)** to ϵ**(a**, ***i'*****)**. This change can affect significantly the energy gap for the virtual transition ***i*** → ***a***. It is important to note that the ***a*** antibonding orbital is not affected by the ***i*** → **BD*** hyperconjugative interaction.

that the main effect of that interaction causes a decrease in that $^1J_{CH}$ SSCC. A similar scheme indicates that a hyperconjugative interaction into the σ^*_{CH} antibond (i.e., $\sigma_{BD} \rightarrow \sigma^*_{CH}$) decreases the J^b contribution to the FC term, and to a lesser extent, to the absolute value of J^{ob}. (σ_{BD} stands for any bond or lone-pair belonging to the compound under study.) If the "other bond" undergoes a hyperconjugative interaction, then a decrease in the absolute value of J^{ob} to the FC term of $^1J_{CH}$ is expected, therefore increasing the FC term of the $^1J_{CH}$ SSCC.

The above qualitative considerations were useful when looking for a set of model compounds where to study the influence of hyperconjugative interactions on $^1J_{CH}$ SSCCs. On these grounds the series **Ia** was chosen since in a previous work it was observed that in these strained compounds very strong hyperconjugative interactions of type $\sigma_{C_iC_3} \rightarrow \sigma^*_{C_1X}$ take place (where C_i stands for any of the three bridge carbon atoms). It should be noted that the three $\sigma_{C_2C_3}$, $\sigma_{C_4C_3}$, and $\sigma_{C_5C_3}$ bonding orbitals participate in three different J^{ob} contributions to $^1J_{C_3H}$; therefore, such hyperconjugative interactions should decrease their absolute values. Consequently, according to the above qualitative considerations, it is expected that these J^{ob} contributions to the FC term should yield an increase in $^1J_{C_3H}$. Therefore, a priori it can be expected that in series **Ia** the $^1J_{C_3H}$ SSCC should show important substituent effects (i.e., positive values for electronegative substituents and negative values for electropositive substituents). In fact, an electronegative substituent should increase such hyperconjugative interactions widening the energy gaps between the $\sigma_{C_2C_3}$, $\sigma_{C_4C_3}$, and $\sigma_{C_5C_3}$ bonds and the $\sigma^*_{C_3H}$ antibond orbital, yielding a decrease in the absolute value of the J^{ob} contributions to the FC term of the $^1J_{C_3H}$ SSCC. The converse holds for an electropositive substituent. It is also observed that interactions of type $\sigma_{C_iC_3} \rightarrow \sigma^*_{C_1X}$ would also affect J^{ob} contributions to $^1J_{CH}$ SSCCs corresponding to bridge carbon atoms like, for instance, $^1J_{C_2H}$. For this reason, compounds of series **Ib** are also included in this study since a comparison of these "lateral" $^1J_{C_2H}$ SSCCs is expected to provide further insight into factors affecting these one-bond couplings. It should be stressed that different effects affecting a given SSCC are in general intertwined, and the inclusion in the present study of this type of couplings could provide indirect evidence about the correctness of conclusions presented in this work.

3. Experimental and Computational Details

A. Experimental Details. Syntheses of compounds of series **Ia** and **Ib** are described elsewhere.[18,24] Samples were prepared in $CDCl_3$ (X = NH_3Cl in D_2O) at concentrations of ca. 0.6 mol/L. ^{13}C NMR spectra were recorded on a Varian Gemini 300BB instrument, operating at 75.462 MHz. $^1J^{13}_{C_1H}$ SSCCs were determined from proton-coupled spectra, measured at 100−500 Hz spectral width, with a digital resolution of ca. 0.1 Hz/point. Experimental couplings thus obtained are considered to be accurate to ± 0.1 Hz (Department of Chemistry, Faculty of Science and Engineering, Flinders University of South Australia).

B. Computational Details. The geometries for 1-X-bicyclo-[1.1.1]pentane (**Ia**) and 1-X-3-methylbicyclo[1.1.1]pentane (**Ib)** derivatives were optimized using the hybrid B3LYP functional, which corresponds to the Lee et al. correlated functional,[25] and the exchange part is treated according to the Becke's three-parameter approach.[26] For such optimizations the 6-311G(d,p) basis set was chosen. The geometries for methane (**II**) and tetrahydropyran (**IV**) were calculated at the MP2/cc-pVTZ level.

Calculations of all four terms of SSCCs (i.e FC, SD, PSO, and DSO) were carried out using the B3LYP functional, and the EPR-III basis set[27] was chosen, which is of a triple-ζ quality and includes diffuse and polarization functions. For compounds containing either a Cl, Br, or I atom, two different basis sets were employed, namely (i) EPR-III for all light atoms and all-electron 6-311** for the halogen atom and (ii) the same for all light atoms and the LANL2DZ ECP for the halogen atom. Since results found with these two different basis sets are similar (see below), for Sn-containing compounds, the latter possibility was chosen. The ***s*** part of the EPR-III basis set is enhanced to better reproduce the electronic density in the nuclear regions; this point is particularly important when calculating the FC term. It is important to stress that coupling constants calculated at the B3LYP/EPR-III level are close to the basis set converged values.[28] The CP-DFT[20] perturbative approach was used for calculating all the three second-order terms of spin−spin couplings (i.e., FC, SD, and PSO); the DSO term is treated as a first-order quantity. All DFT calculations were carried out with the Gaussian 03 package of programs.[21] Hyperconjugative interactions were studied using the NBO approach.[22]

For studying electrostatic effects, the FC term of $^1J_{CH}$ SSCCs were calculated for methane (**II**), 1-X-bicyclo[1.1.1]pentanes (X = H and F) (**III**), and tetrahydropyran (**IV**) including a charge *q* facing a σ_{CH} bond (C—H- - -*q*); in all cases the H- - - *q* distance was kept fixed at 2.5 Å. The point charge *q* was changed in the range −0.5 au to +0.5 au in 0.1 au steps. These model systems correspond to an inhomogeneous electric field directed along the C—H bond and pointing in the C → H direction. This electrostatic interaction mimics somehow the main interaction that takes place in weak hydrogen bonds of type C—H- - -X (electronegative atom) giving place to the so-called "blue-shifting hydrogen bonds"[14a−d] and yields a slight shortening to the corresponding σ_{CH} bond. It is also known that such an interaction can be detected experimentally, measuring the corresponding $^1J_{CH}$ SSCC, and it manifests itself as an increase of a few Hz. It should be recalled that such an increase in a $^1J_{CH}$ coupling could be reproduced by theoretical calculations at the ab initio HF and post-HF levels as well as within the DFT framework.[5d]

4. Results and Discussion

A. $^1J_{CH}$ SSCCs in Series Ia and Ib. In Table 1, experimental $^1J_{C_3H}$ and $^1J_{C_2H}$ (= $^1J_{C_4H}$ = $^1J_{C_5H}$) SSCCs in 24 members of series **Ia** (Scheme 1) are displayed. It is observed that the range of values covered by $^1J_{C_3H}$ SSCCs goes from 156.3 to 181.2 Hz, while $^1J_{C_2H}$ SSCCs cover a range from 143.4 to 151.6 Hz. In Table 1 are shown also experimental values of $^1J_{C_2H}$ SSCCs in 16 members of series **Ib** (Scheme 1); they cover a range from143.2 Hz to 150.0 Hz. Substituent effect trend for $^1J_{C_3H}$ SSCCs does not parallel exactly that of $^1J_{C_2H}$ SSCCs in **Ia**.

TABLE 1: Experimental $^1J_{CH}$ Couplings in 1-X-Bicyclo[1.1.1]pentanes, Ia, and in 1-X-3-Methylbicyclo[1.1.1]pentanes, Ib

	Ia		Ib
	$^1J_{C_3H}$	$^1J_{C_2H}$	$^1J_{C_2H}$
H	167.8	144.5	146.8
CH_3	163.9	146.7	
CH_2OH	165.5	144.2	143.5
t-Bu	n.o.	143.4	
Ph	165.4	144.4	143.7
$COCH_3$	167.0	on[a]	
$CONH_2$	167.0	146.3	
CO_2H	168.3	147.5	146.6
CO_2CH_3	168.0	147.5	146.3
CN	170.6	149.1	148.2
NH_2	169.6	144.4	143.2
NH_3Cl	178.1	148.6	147.4
NO_2	180.4	151.6	150.0
OCH_3	174.2	145.4	
OAc	176.4	147.6	146.8
F	181.2	148.6	
Cl	177.0	149.2	147.9
Br	176.7	149.8	148.4
I	174.1	149.7	148.5
SPh	169.8	147.0	146.3
SO_2Ph	174.0	150.3	149.2
SePh	169.4	147.5	146.4
$SnBu_3$	156.3	143.8	
$SnPh_3$	159.9	144.9	

[a] Not observed.

SCHEME 1: 1-X-Bicyclo[1.1.1]pentane (Ia) and 1-X-3-methylbicyclo[1.1.1]pentane (Ib).

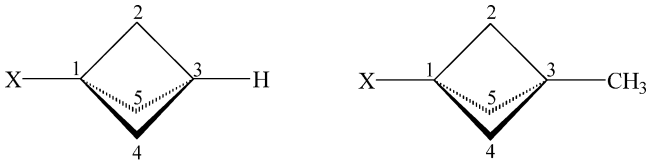

Ia **Ib**

For "linear" X substituents the direction defined by both bridgehead carbon atoms in **Ia** corresponds to a 3-fold symmetry axis; consequently, all six "lateral" $^1J_{CH}$ SSCCs are equal. Experimentally, for nonlinear substituents similar effective symmetries were observed both in **Ia** and **Ib**, which is indicative that in all cases different rotamers are separated by a rather low potential energy barrier. For a selected set of compounds displayed in Table 1, $^1J_{CH}$ SSCC and NBO calculations were performed. Calculated $^1J_{CH}$ SSCCs are compared with their experimental values in Table 2, where all four isotropic terms are included, although they are not explicitly shown. In all cases noncontact terms are notably smaller than the FC term; they cover the following ranges, SD (0.4 ± 0.05) Hz; PSO from 0.4 to 0.6 Hz; and DSO from 0.8 to 1.1 Hz. For compounds involving Cl, Br, or I, two different types of SSCC calculations were carried out, namely, EPR-III for light atoms and for the halogen atom these two different choices were made, all-electron 6-311G** basis set and the ECP LANL2DZ. As shown in Table 2, there is no much difference between them, for this reason in tin-containing compounds only the second alternative was used (i.e., LANL2DZ ECP for the heavy atom while the EPR-III basis set was used for light atoms). Experimental trends are nicely reproduced, although calculated total $^1J_{C_3H}$ SSCCs are in general overvalued from about 5 to 7 Hz, a trend that is similar to that observed in other calculated $^1J_{CH}$ couplings.[5d] This overvaluation worsens when taking into account the effect of nuclear motions, which is now accepted to be dominated by the zero-point vibrational correction (ZPVC).[29] For $^1J_{C_2H}$ SSCCs such an overvaluation is somewhat smaller than for $^1J_{C_3H}$ SSCCs. However, calculated couplings follow nicely the experimental trends, which are taken as an evidence that interactions that define experimental trends are well accounted for at the level of theory used in this work.

TABLE 2: Comparison between Calculated and Experimental $^1J_{C_3H}$ in Ia and $^1J_{C_2H}$ SSCCs for a Selected Set of the Substituents Shown in Table 1

	Ia		Ia		Ib	
	$^1J_{C_3H}$		$^1J_{C_2H}$		$^1J_{C_2H}$	
X	exp	calcd	exp	calcd	exp	calcd
H	167.8	168.5	144.5	148.5	146.8	147.8
CH_2OH	165.5	171.2	144.2	149.0	143.5	148.1
$COCH_3$	167.0	172.6	no[a]	150.9	145.8	150.0
$CONH_2$	167.0	173.8	146.3	151.8	no	150.1
COOH	168.3	173.8	147.5	151.8	146.6	151.0
CN	170.6	175.0	149.1	153.2	148.2	152.2
NH_2	169.6	175.2	144.4	148.4	143.2	147.6
NO_2	180.4	184.3	151.6	155.0	150.0	154.0
F	181.2	186.2	148.6	151.7		
Cl[b]	177.0	182.9	149.2	153.5	147.9	152.5
Br[b]	176.7	182.6	149.8	154.0	148.4	153.0
I[b]	174.1	180.5	149.7	154.3	148.5	153.2
Cl[c]	177.0	183.5	149.2	153.4	147.9	152.4
Br[c]	176.7	182.2	149.8	153.8	148.4	152.8
I[c]	174.1	180.9	149.8	154.0	148.5	153.0
$SnMe_3$	*d*	163.2	*e*	148.3		

[a] Not observed. [b] Calculations of SSCCs were performed using the B3LYP/EPR-III basis set for all atoms except Cl, Br, and I where the 6-311G** basis set was employed. [c] Calculations of SSCCs were performed using the B3LYP/EPR-III basis set for all atoms except Cl, Br, I, and Sn where the LANL2DZ ECP was employed. [d] In X = $SnBu_3$, $^1J_{C_3H}$ = 156.3 Hz and in X = $SnPh_3$, $^1J_{C_3H}$ = 159.9 Hz. [e] In X = $SnBu_3$, $^1J_{C_2H}$ = 143.8 Hz and in X = $SnPh_3$, $^1J_{C_2H}$ = 144.9 Hz.

A-1. $^1J_{C_3H}$ SSCCs in Series Ia. NBO calculations were carried out for compounds displayed in Table 2, and relevant NBO parameters are analyzed to verify how consistent are the qualitative considerations made above with calculated FC contributions in members of series **Ia**. NBO occupancies are considered to be significant parameters to estimate the importance of different hyperconjugative interactions involving either a bond or an antibond, which must affect, according to Section 2**,** $^1J_{C_3H}$ *SSCCs*. It is to be noted that, for the problem under study, such occupancies are considered to be more significant parameters than individual hyperconjugative interactions since for instance, according to Section 2, all hyperconjugative interactions from the $\sigma_{C_2C_3}$, $\sigma_{C_4C_3}$, and $\sigma_{C_5C_3}$ "other bonds" ($\sigma_{C_iC_3}$, when quoted together) irrespective of the acceptor antibonding orbital. The same holds for other occupancies considered in this section. In Table 3, orbital occupancies relevant to study qualitatively the behavior of J^b (σ_{C_3H} bond and of the $\sigma^*_{C_3H}$ antibond) and J^{ob} ($\Sigma\sigma_{C_iC_3}$ bond orbitals) contributions to the FC term of $^1J_{C_3H}$ SSCCs are displayed. Bond occupancies are given as the difference between the actual calculated values and the "ideal" occupation of a bonding orbital (i.e., 2.000); for all occupancies only three decimal figures are kept and are given in 10^{-3} units. Within this approximation, for nonlinear substituents, the occupancies of all three $\sigma_{C_2C_3}$, $\sigma_{C_4C_3}$, and $\sigma_{C_5C_3}$ bonds are the same. Referring to the FC term of $^1J_{C_3H}$ SSCCs, the former two occupancies convey an idea of how the J^b contribution is affected by the X substituent. On the other hand, the latter three occupancies ($\sigma_{C_2C_3}$, $\sigma_{C_4C_3}$, and $\sigma_{C_5C_3}$) convey an idea of how the three J^{ob} contributions are affected by the X substituent effect. In the same Table 3 are included the experimental $^1J_{C_3H}$ SSCCs, (E), and the calculated FC contribu-

TABLE 3: Calculated FC Term of $^1J_{C_3H}$ SSCCs, Occupancies of NBO Orbitals Relevant for Analyzing the $^1J_{C_3H}$ SSCC Values, the s % Character at the C Atom of the σ_{C_3H} Bond, and the NBO Atomic Charge at the C_1 Atom (au)[a]

	H	$SnMe_3$	CH_3	CH_2OH	$COCH_3$	$CONH_2$	COOH	CN	NH_2	NO_2	F	Cl	Br	I
σ_{C_3H}	−6	−7	−6	−6	−6	−6	−6	−6	−7	−10	−10	−15	−16	−18
$\sigma^*_{C_3H}$	39	45	39	39	39	38	37	35	36	36	35	38	40	42
$\Sigma\sigma_{C_{2,4,5}C_3}$	−111	−117	−120	−120	−120	−120	−120	−123	−129	−150	−156	−168	−171	−174
$^1J_{C_3H}$ (E)[b]	167.8	159.9[c]	163.9	165.5	167.0	167.0	1.683	170.6	169.6	180.4	181.2	177.0	176.7	174.1
$^1J_{C_3H}$ (T)[d]	167.5	161.7	169.0	169.7	171.1	172.2	172.2	173.5	173.6	182.8	184.6	181.3	181.0	179.0
s %	28.95	28.12	28.87	28.87	29.03	29.12	29.19	29.48	29.09	29.37	29.48	28.63	28.24	27.90
Q_1 (10^{-3})	−173	−525	2	−25	−111	−129	132	−152	188	86	412	−31	−91	−181

[a] Bond occupancies are given as the difference between the actual calculated values and the "ideal" occupation, 2.000; for all occupancies only three decimal figures are kept and are given in 10^{-3} units. [b] Experimental values, taken from Table 1. [c] Measured for X = $SnPh_3$. [d] Calculated values for the FC contribution.

TABLE 4: Occupancies of One Antibonding and Four Bonding Orbitals Defining the J^b and J^{ob} Contributions to the FC Term of $^1J_{C_2H}$ SSCCs in Six Members of Series Ia Having the C_1- -C_3 Direction as a 3-Fold Symmetry Axis[a]

	X = H	CN	F	Cl	Br	I
σ_{C_2H}	−9	−9	−10	−10	−10	−10
$\sigma^*_{C_2H}$	19	18	18	18	18	18
$\sigma_{C_1C_2}$	−37	−58	−36	−38	−38	−37
$\sigma_{C_2C_3}$	−37	−41	−52	−56	−57	−58
$^1J_{C_2H'}$(E)	144.5	149.1	148.6	149.2	149.8	149.7
$^1J_{C_2H}$(T)	148.5	153.2	151.7	153.4	152.8	154.0
s %	25.74	26.00	26.13	25.86	25.80	25.75

[a] Occupancies are given as in Table 3.

tion, (T), to the $^1J_{C_3H}$ coupling; the NBO s % character of the σ_{C_3H} bond at C_3 and the natural atomic charge (Q_1) at the C_1 carbon atom. It should be recalled that the s % character affects the "perturbator" at C_3, while Q_1 conveys an idea of how important an electrostatic substituent effect could be. It is observed that Q_1 and the s % character of the σ_{C_3H} bond at C_3 do not correlate with each other. Although it is expected that hyperconjugative interactions should affect the C_3 s % character, an electric field along the σ_{C_3H} bond could also affect it even if hyperconjugative interactions are not much affected.[5c]

Values displayed in Table 3 show that the occupancy of the σ_{C_3H} bond is not sensitive to substitution for X groups having a carbon atom at the α position. For those X substituents changes in the occupancies of $\sigma_{C_iC_3}$ bonds are compatible with the decrease, in absolute value, of the three J^{ob} contributions, yielding a slightly larger calculated FC term for the $^1J_{C_3H}$ SSCC than for X = H. The negative substituent effect observed for X = $SnMe_3$ seems to originate mainly (see Section 2) in the J^b contribution owing to hyperconjugative interactions into the $\sigma^*_{C_3H}$ antibonding orbital. For X = CN and X = NH_2, the calculated FC terms are practically the same; it seems that this result is a consequence of different competitive effects, for instance, J^b(X = CN) > J^b(X = NH_2); $|J^{ob}$(X = CN)| > |J^{ob}(X = NH_2)| and the s % character at C_3 of the σ_{C_3H} bond is larger for X = CN than for X = NH_2. The $^1J_{C_3H}$ trend along the halogen atoms is also very interesting since the σ_{C_3H} occupancy decreases while that of $\sigma^*_{C_3H}$ increases, defining a decrease of J^b along the series. On the other hand, the $\sigma_{C_iC_3}$ occupancies decrease yielding a decrease, in absolute value, in J^{ob}, and the s % character at C_3 decreases along this series.

A-2. "Lateral" $^1J_{CH}$ SSCCs in Series Ia and Ib. In Table 4, the occupancies of the σ_{C_2H} bonding and of the $\sigma^*_{C_2H}$ antibonding orbitals as well as of those of $\sigma_{C_1C_2}$ and $\sigma_{C_2C_3}$ bonds are displayed for compounds with X = H, CN, F, Cl, Br, and I. With the exception of X = NH_2 and X = NO_2 (see below), for other compounds the differences in the lateral $^1J_{CH'}$ SSCC are small, and it is not worth commenting on them. Since compounds shown in Table 4 have a 3-fold symmetry axis, all six lateral $^1J_{CH}$ SSCCs are the same. In this Table 4 are also included the experimental $^1J_{C_2H}$ SSCCs, (E), and the calculated FC contribution, (T), to the corresponding $^1J_{C_2H}$ coupling. The s % characters at the C_2 carbon atom of the σ_{C_2H} bonds are also displayed. In these compounds there are three different J^{ob} contributions to the FC term of the $^1J_{C_2H'}$ SSCC, namely, those corresponding to the $\sigma_{C_2H'}$ bond (i.e., to the σ_{C_2H} bond not containing the coupling proton), and those corresponding to the $\sigma_{C_1C_2}$ and $\sigma_{C_2C_3}$ bonds. The X = CN substituent effect on $^1J_{C_2H}$ is compatible with smaller absolute values than for X = H of the J^{ob} contributions corresponding to the $\sigma_{C_1C_2}$ and $\sigma_{C_2C_3}$ bonds since their occupancies are smaller than for X = H. For X = F, Cl, Br, and I, while the occupancies of the $\sigma_{C_1C_2}$ bonds are practically the same as that for X = H, those of the $\sigma_{C_2C_3}$ bonds are notably smaller. This trend is compatible with a decrease of the absolute value of the J^{ob} contribution, where ob = $\sigma_{C_2C_3}$ and originates in the increasing acceptor ability along the antibond series $\sigma^*_{C_1F} < \sigma^*_{C_1Cl} < \sigma^*_{C_1Br} < \sigma^*_{C_1I}$. It is noted that, along the halogen series, while $^1J_{C_3H}$ decreases, $^1J_{C_2H'}$ does not change much.

TABLE 5: Calculated FC Contributions to "Lateral" $^1J_{C_iH_j}$ SSCCs in Compounds I (X = NH_2) and I (X = NO_2)[a]

	NH_2			NO_2		
	$^1J_{C_2H_9}$	$^1J_{C_4H_{10}}$	$^1J_{C_4H_{11}}$	$^1J_{C_2H_9}$	$^1J_{C_4H_{10}}$	$^1J_{C_4H_{11}}$
FC	146.2	145.3	148.1	153.1	151.8	155.0
$\sigma_{C_iH_j}$	−9	−10	−10	−10	−10	−10
$\sigma^*_{C_iH_j}$	19	20	19	17	17	17
$\sigma_{C_iH_j}$(ob)	−9	−10	−10	−10	−10	−10
$\sigma_{C_1C_i}$	−40	−46	−46	−40	−54	−54
$\sigma_{C_3C_i}$	−42	−41	−41	−50	−50	−50
s %	25.62	25.35	25.68	26.06	25.97	26.23

[a] Occupancies of bonds and antibonds affecting the J^b and J^{ob} of such SSCCs are also shown; they are given as in Table 3. The spatial orientation of the 6 lateral σ_{CH} bonds, and the X groups are displayed in Figure 2.

The calculated FC terms of "lateral" $^1J_{CH}$ SSCCs in compounds **Ia** (X = NH_2) and **Ib** (X = NO_2) are worthy of considering in detail. Their values are displayed in Table 5, where occupancies of bonds and antibonds relevant for the qualitative analysis of their J^b and J^{ob} orbital contributions as well as the s % character at the C atom of each bond are shown; occupancies are expressed as in Table 3. The spatial orientation of the 6 lateral σ_{CH} bonds and the X groups are displayed in Figure 2, where the axial view from X of both compounds are shown. For **Ia** (X = NH_2) (Figure 2a), the N nonbonding electron pair is in the symmetry plane, while for **Ib** (X = NO_2) both O═N bonds are contained in that plane. In both compounds the FC term of $^1J_{C_4H_{11}}$ is larger than the FC term of $^1J_{C_4H_{10}}$, probably due to the proximity of H_{11} to an electronegative atom, N for NH_2, and O for NO_2.[5c] It is noted that occupancies of relevant bonds and antibonds for X = NO_2 are the same for

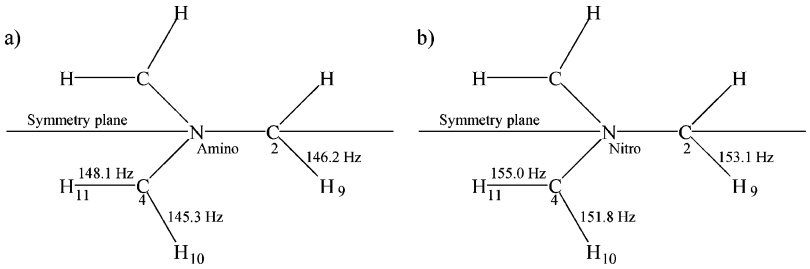

Figure 2. Axial view for (a) **Ia** (X = NH_2) and (b) **Ia** (X = NO_2). In both cases the calculated FC contribution for the lateral $^1J_{CH}$ SSCCs is shown.

TABLE 6: FC Terms of SSCCs (in Hz) Calculated in the Model Systems IIa and IIb When *q* Changes from −0.5 to +0.5 au[a]

	IIa					IIb				
q	$^1J_{CH_a}$	$^1J_{CH}$	s %	σ_{CH_a}	$\sigma^*_{CH_a}$	$^1J_{CH_a}$	$^1J_{CH}$	s %	σ_{CH_a}	$\sigma^*_{CH_a}$
−0.5	137.0	123.0	25.77	−1.5	0.6	192.2	108.9	32.98	−1.2	0.5
0.0	126.7	126.7	25.00	−1.2	0.4	180.4	113.2	32.06	−1.0	0.5
0.5	115.6	131.0	24.21	−1.0	0.2	167.0	117.9	31.14	−0.9	0.4

[a] Occupancies of σ_{CH} bond and σ^*_{CH} antibond are given as in Table 3.

SCHEME 2: IIa *d* = 2.5 Å; *q* Was Changed from −0.5 to +0.5 au[a]

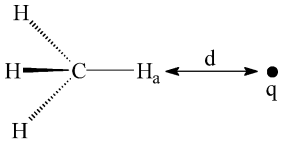

II

[a] The structure of the CH_4 molecule was kept fixed at its optimized geometry. **IIb** the Same as in **IIa**, but the H−C−Ha angle was changed from tetrahedral to 120°.

$\sigma_{C_4H_{10}}$ and $\sigma_{C_4H_{11}}$ bonds; however, their respective s % character at C_4 show significant differences, 25.97% and 26.23%, respectively. Although the relevant energy gaps could also be affected by this electrostatic interaction, it seems that the larger effect comes through the "perturbators", due to changes in the s % character, rendering a larger FC contribution for $^1J_{C_4H_{11}}$ than for $^1J_{C_4H_{10}}$. The small difference in the occupancy of the corresponding antibond for X = NH_2 is too small to account for the observed difference on the FC term. Therefore, differences in $^1J_{C_4H_{11}}$ and $^1J_{C_4H_{10}}$ SSCCs are interesting examples of couplings affected by electrostatic effects not affecting the relevant hyperconjugative interactions.

Differences in $^1J_{C_2H}$ SSCCs for analogous compounds of series **Ia** and **Ib** are commented in Section 4E, where they are rationalized in terms of differences in their respective geometries as given by the bridgehead C_1- - -C_3 distance.

B. Electrostatic Effects on $^1J_{CH}$ SSCCs Studied in Model Systems. In the previous section, it was argued that the calculated differences for the FC contribution to $^1J_{C_4H_{11}}$ and $^1J_{C_4H_{12}}$ SSCCs in compounds **Ia** (X = NH_2) and **Ia** (X = NO_2) originate in an electrostatic effect due to the proximity of the $\sigma_{C_4H_{11}}$ bond to an electronegative atom (N for X = NH_2; O for X = NO_2). To deepen the understanding of such an effect, NBO and FC SSCC calculations were carried out in the model system **IIa** (Scheme 2) (i.e., a CH_4 molecule with a point charge facing one of its σ_{CH} bonds). The H_a- - -*q* distance was fixed at 2.5 Å, with *q* covering a range from −0.5 au to +0.5 au in 0.1 au steps, and the CH_4 geometry was fixed at its optimized structure (*q* = 0 au). This system is chosen since in methane very small hyperconjugative interactions take place; therefore, electrostatic interactions on them should not be important. As expected, occupancies of both σ_{CH_a} and $\sigma^*_{CH_a}$ orbitals changed less than 0.001; on the other hand, the FC term of $^1J_{CH_a}$ increases almost linearly from *q* = +0.5 to *q* = −0.5 au, though the sensitivity to a positive charge is slightly larger than for a negative charge.

The main results thus found are collected in Table 6, where it is observed that $^1J_{CH_a}$ SSCC changes 21.4 Hz when *q* changes from +0.5 au to −0.5 au, while for the remaining bonds $^1J_{CH}$ changes in −8.0 Hz within the same range of *q* values. It is important to stress that in **IIa** only weak hyperconjugative interactions take place, and for this reason, changes in occupancies are too small. To verify if the electrostatic effect observed in **IIa** is sensitive to the s % character of the σ_{CH} bond facing charge *q*, the same calculations were repeated for **IIb** (Scheme 1) (i.e., for **IIa** changing the H−C−H_a angles from tetrahedral to 120° but keeping the C−H_a direction as a 3-fold symmetry axes). In these conditions $^1J_{CH_a}$ changes 25.2 Hz when *q* changes from +0.5 to −0.5 au (i.e., the sensitivity to electrostatic interactions seems to increase somewhat when increasing the s % character at the C atom). Such a distortion in the CH_4 molecule changes the FC term of $^1J_{CH}$ SSCC (for *q* = 0 au) from 126.7 to 180.4 Hz, and the s % character at the C atom changes from 25.0% to 32.06%.

To study how different is the influence of the same electrostatic interaction, shown in the model system **II**, when applied to a system undergoing strong σ-hyperconjugative interactions, models **IIIa** and **IIIb** are chosen (Scheme 3). The

SCHEME 3: *d* = 2.5 Å; *q* Was Changed from −0.5 to +0.5 au[a]

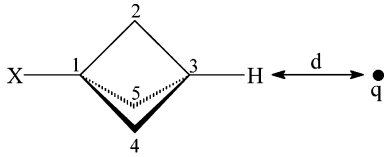

III

[a] X = H (**IIIa**), X = F (**IIIb**).

distance *d* and charge *q* were fixed as in model **II** (i.e., 2.5 Å), and *q* was changed from +0.5 to −0.5 au. Results for these two model systems are displayed in Table 7, where it is observed that in **IIIa** and **IIIb** $^1J_{C_3H}$ changes in 30.6 and 31.2 Hz, respectively, when changing from *q* = +0.5 to *q* = −0.5. Those ranges for $^1J_{C_3H}$ SSCCs in **IIIa** and **IIIb** should be compared with those in methane, **IIa** and **IIb**, (i.e., 21.4 and 25.2 Hz, respectively, as shown in Table 6).

In **IIIa** and **IIIb** the behavior of the $\sigma^*_{C_3H}$ antibonding orbital occupancy is consistent with an inhibition of hyperconjugative interactions into this antibond when *q* < 0, and with an

TABLE 7: FC Terms of SSCCs (in Hz) Calculated in Model Systems IIIa and IIIb for Different Point Charges Facing the σ_{C_3H} Bond[a]

	IIIa					IIIb				
q	$^1J_{C_3H}$	s %	σ_{C_3H}	$\sigma^*_{C_3H}$	$\sigma_{C_2C_3}$	$^1J_{C_3H}$	s %	σ_{C_3H}	$\sigma^*_{C_3H}$	$\sigma_{C_2C_3}$
−0.5	181.2	29.91	−7	34	−39	197.6	30.12	−14	31	−54
0.0	166.5	28.86	−6	39	−37	182.9	29.31	−12	35	−52
0.5	150.6	27.59	−5	47	−36	166.4	28.30	−10	41	−50

[a] Occupancies of σ_{C_3H} and $\sigma_{C_2C_3}$ bonds and $\sigma^*_{C_3H}$ antibonds are given as in Table 3. The s % character of the σ_{C_3H} bond at the C_3 carbon atom is also shown.

SCHEME 4

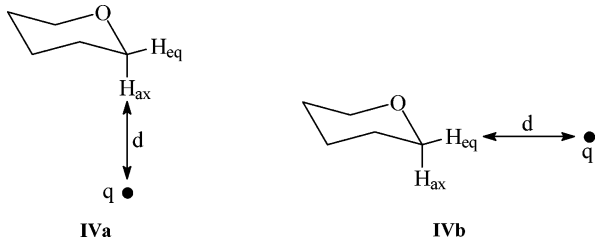

enhancement of such interactions when $q > 0$. According to the qualitative description presented in Section 2, electrostatic induced changes in the $\sigma^*_{C_3H}$ occupancy are compatible with an increase in the J^b contribution to the FC term of $^1J_{C_3H}$ when the σ_{C_3H} bond faces a negative charge. The occupancy of the σ_{C3H} bond for different values of q show that the proximity to a negative charge enhances hyperconjugative interactions from a σ_{CH} bond, counteracting in part the effect on J^b. Changes in the occupancies of $\sigma_{C_iC_3}$ bonds ($i = 2, 4, 5$) are very important, and they show that such a negative charge facing the σ_{C3H} bond enhances hyperconjugative interactions of type $\sigma_{C_iC_3} \rightarrow \sigma^*_{C_1X}$. These interactions, according to Section 2, yield algebraic increases in the J^{ob} contributions to the FC term of $^1J_{C_3H}$ SSCC. The s % character at C_3 of the σ_{C_3H} bond is more sensitive to electrostatic interactions for **IIIa** than for **IIIb**; the former changes 2.32% while the latter 1.82% when changing q from +0.5 to −0.5 au. These values should be compared with those in methane, where the s % character changes in 1.56% for the same change in q. Taking into account the NBO Q_1 values (Table 3), it seems that the point charge q tends to compensate the electrostatic effect of Q_1 on the FC term of the $^1J_{C_3H}$ SSCC; in fact, in **IIIb** Q_1 changes from 0.412 au for $q = 0$ to 0.406 au for $q = -0.5$ au. One of the important questions that remain to be answered is about the larger sensitivity to the q electrostatic effect of the FC term of $^1J_{C_3H}$ SSCC in **IIIa** and **IIIb** than that of $^1J_{CH}$ in both **IIa** and **IIb**. In the next subsection, an answer to such a question is sought by studying this type of electrostatic interaction on a σ_{CH} bond participating in a strong negative hyperconjugative interaction.

C. Negative Hyperconjugative Interaction Effect on $^1J_{CH_{ax}}$ and on $^1J_{CH_{eq}}$ in Tetrahydropyran (IV). In Section 4B, it was observed that in **IIIa** and **IIIb** the sensitivity of $^1J_{C_3H}$ SSCC to charge q is notably different to that observed in **II**. Apparently, this originates in the strong hyperconjugative interactions that take place in the bicyclo[1.1.1]pentane substrate, where both J^b and J^{ob} contributions to $^1J_{C_3H}$ are strongly affected by charge q. For this reason, it is considered interesting to test two other systems, **IVa** and **IVb** (Scheme 4), to study the electrostatic effect on $^1J_{CH}$ SSCCs in tetrahydropyran with a point charge q facing the $\sigma_{C_1H_{ax}}$ bond, **IVa**, and with a point charge q facing the $\sigma_{C_1H_{eq}}$ bond, **IVb**. Both distance d and charge q were taken as in model systems **II** and **III**. In **IV** there is a strong negative hyperconjugative interaction into the $\sigma^*_{C_1H_{ax}}$ and the pyran substrate is notably less strained than those of models **IIIa** and **IIIb**. Calculated FC terms of $^1J_{CH_{ax}}$ and $^1J_{CH_{eq}}$ SSCCs; the s % character at the C atom of the respective σ_{CH} bond, and the occupancies of bonds and antibonds that affect the respective J_b and J^{ob} contributions (for $q = -0.5$, 0.0, and +0.5 au) are collected in Table 8.

It is observed that, when changing q from +0.5 au to −0.5 au, the FC terms of $^1J_{CH_{ax}}$ (**IVa**) and $^1J_{CH_{eq}}$ (**IVb**) SSCCs change in 20.9 and 21.5 Hz, respectively. Comparing results displayed in Tables 7 and 8 ,it is noteworthy that, while in systems **IIIa** and **IIIb** the occupancies of bonds affecting the J^{ob} contributions are notably changed, in **IVa** and **IVb** they are not affected by the presence of point charge q. This result is somewhat unexpected since the $\sigma_{C_1H_{ax}}$ bond is playing the role of "other bond" in **IVb**, and the electrostatic interaction affecting $\sigma_{C_1H_{eq}}$ does not change, within the approximation considered here, the $\sigma_{C_1H_{ax}}$ occupation. This different behavior and the large natural charge Q_1 at the C_1 atom, seem to be the main reasons why $^1J_{C_3H}$ in **IIIa** and **IIIb** is more sensitive to electrostatic interactions than both $^1J_{CH_{ax}}$ and $^1J_{CH_{eq}}$ in **IVa** and **IVb**, respectively. In Figure 3, the behaviors of $^1J_{CH_{ax}}$ and $^1J_{CH_{eq}}$ SSCCs with a point charge facing the respective σ_{CH} bonds are displayed. In Figure 3a, the second-order perturbation energy corresponding to the $n(O) \rightarrow \sigma^*_{C_1H_{ax}}$ negative hyperconjugative interaction and the calculated FC term of $^1J_{C_1H_{ax}}$ versus the point charge q are displayed, while in Figure 3b the second-order perturbation energy corresponding to the $\sigma_{C_3O} \rightarrow \sigma^*_{CH_{eq}}$ hyperconjugative interaction and the calculated FC term of $^1J_{C_1H_{eq}}$ versus the point charge q are plotted. In both cases a negative point charge facing the corresponding σ_{CH} bond inhibits the respective hyperconjugative interaction into the σ^*_{CH} antibond; however, it is important to note the different vertical scale used in Figure 3a,b for the second-order perturbation energy. This conspicuous difference between both hyperconjugative interactions suggests that, changes in $^1J_{C_1H_{ax}}$ are mainly due to the inhibition of the $n(O) \rightarrow \sigma^*_{C_1H_{ax}}$ interaction when a negative charge faces the $\sigma_{C_1H_{ax}}$ bond. On the other hand, results displayed in Figure 3 suggest that changes in the $^1J_{C_1H_{eq}}$ SSCC plotted in Figure 3b originate mainly on changes in the electronic distribution along the $\sigma_{C_1H_{eq}}$ bond produced by the electrostatic interaction with the point charge q. This effect seems to be similar to that described above for **IIa**, where hyperconjugative interactions are very weak.

D. Oxygen Protonation Effect on $^1J_{CH_{ax}}$ and $^1J_{CH_{eq}}$ SSCCs in Tetrahydropyran (IVc). In model **IVc** (Scheme 5) tetrahy-

TABLE 8: FC Term of $^1J_{CH_{ax}}$ and $^1J_{CH_{eq}}$ SSCCs in Model Systems IVa and IVb for Different Point Charges Facing the $\sigma_{CH_{ax}}$ and $\sigma_{CH_{eq}}$ Bonds, Respectively[a]

	IVa							IVb						
q	$^1J_{CH_{ax}}$	s %	$\sigma_{CH_{ax}}$	$\sigma^*_{CH_{ax}}$	$\sigma_{CH_{eq}}$	σ_{C_1O}	$\sigma_{C_1C_6}$	$^1J_{CH_{eq}}$	s %	$\sigma_{CH_{eq}}$	$\sigma^*_{CH_{eq}}$	$\sigma_{CH_{ax}}$	σ_{C_1O}	$\sigma_{C_1C_6}$
−0.5	146.7	24.48	−14	26	−18	−10	−14	155.5	24.55	−20	16	−13	−10	−14
0.0	136.9	23.76	−13	32	−18	−10	−14	145.8	23.84	−18	18	−13	−10	−14
0.5	125.8	22.93	−12	41	−16	−10	−14	134.0	23.03	−16	21	−12	−10	−14

[a] Occupancies are given as in Table 3.

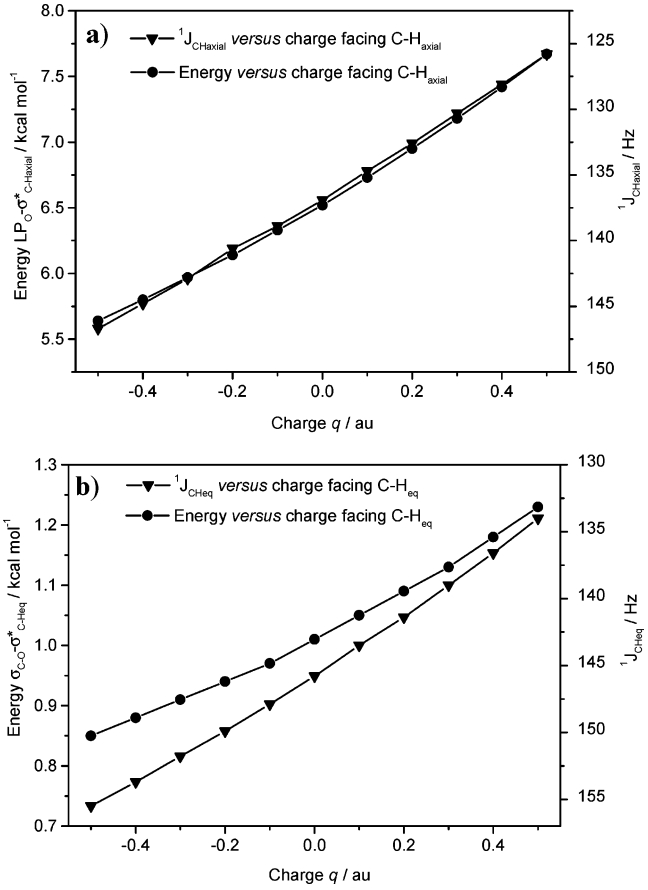

Figure 3. Response of the FC term of $^1J_{CH}$ SSCCs in **IVa** and **IVb** to a point charge q facing the corresponding σ_{CH} bond. In both cases, the H- - -q distance was kept fixed at 2.5 Å, and the tetrahydropyran geometry was kept fixed at its optimized value. (a) In **IVa** the second-order perturbation energy corresponding to the $n(O) \rightarrow \sigma^*_{CHax}$ negative hyperconjugative interaction and the calculated FC term of $^1J_{CHax}$ vs the point charge q. (b) In **IVb** the second-order perturbation energy corresponding to the $\sigma_{C_3O} \rightarrow \sigma^*_{CHax}$ hyperconjugative interaction and the calculated FC term of $^1J_{CHeq}$ vs the point charge q.

SCHEME 5

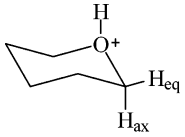

IVc

TABLE 9: Effects upon Protonation of One Oxygen Lone-Pair in Tetrahydropyran

		$^1J_{CH}$	s %	σ_{CH}	σ^*_{CH}	σ_{C_1O}	$\sigma_{C_1C_6}$
ax	neut.	136.9	23.76	−13	32	−10	−14
	prot.	160.7	25.08	−19	19	−7	−12
eq	neut.	145.8	23.84	−13	18	−10	−14
	prot.	151.6	24.04	−18	14	−7	−12

[a] The FC term of SSCCs are given in Hz. s % corresponds to the character of the respective σ_{CH} bond. Occupancies of NBO orbitals, given as in Table 3, relevant to analyze qualitatively the behavior of J^b and J^{ob} contributions to the respective FC terms are shown.

dropyran is protonated with a proton in axial position, where the optimized geometry for neutral hydropyran was held fixed. In Table 9, data corresponding to the FC contribution to $^1J_{CH_{ax}}$ and $^1J_{CH_{eq}}$ SSCCs, the s % character at the C atom of $\sigma_{CH_{ax}}$ and $\sigma_{CH_{eq}}$ bonds, and occupancies of orbitals relevant for analyzing qualitatively the behavior of J^b and J^{ob} contributions to such SSCCs are collected.

TABLE 10: Comparison of Experimental $^1J_{C_2H}$ Couplings (in Hz), Bridgehead C_1- - -C_3 Distances, $d_{C_1C_3}$ (in Å), and $\Delta(d_{C_1C_3})$ (in 10^{-3} Å), and the C_2 s % Character of the σ_{C_2H} Bond

		Ia	Ib		
X	$\Delta(^1J_{C_2H})$	$d_{C_1C_3}$	$d_{C_1C_3}$	$\Delta(d_{C_1C_3})$	Δ(s %)
H	−2.3	1.8812	1.8891	−7.9	0.35
CH_2OH	0.7	1.8821	1.8902	−8.1	0.37
$COCH_3$		1.8820	1.8902	−8.2	0.39
$CONH_2$		1.8818	1.8904	−8.6	0.39
CO_2H	0.9	1.8771	1.8850	−7.9	0.39
CN	0.9	1.8815	1.8898	−8.3	0.37
NH_2	1.2	1.8801	1.8881	−8.2	0.42
NO_2	1.6	1.8398	1.8489	−9.1	0.38
Cl	0.7	1.8403	1.8499	−9.6	0.41
Br	1.4	1.8386	1.8486	−10.0	0.42
I	1.2	1.8398	1.8507	−10.9	0.37

Upon protonation, both $\sigma_{CH_{ax}}$ and $\sigma_{CH_{eq}}$ bond occupancies decrease notably; the former due to the presence of the σ^*_{OH} antibond (i.e., there is an important $\sigma_{CH_{ax}} \rightarrow \sigma^*_{OH}$ interaction) and the latter due to the increase in the acceptor ability of the $\sigma^*_{OC_3}$ antibond. On the other hand, the occupancies of $\sigma^*_{CH_{ax}}$ and $\sigma^*_{CH_{eq}}$ antibonds are notably reduced, although this effect, as expected, is much stronger in the former than in the latter. To understand the behavior of $^1J_{CH_{ax}}$ and $^1J_{CH_{eq}}$ SSCCs upon protonation it is important to remember that the $\sigma_{CH_{ax}}$ bond plays the role of "other bond" for $^1J_{CH_{eq}}$ and so does $\sigma_{CH_{eq}}$ for $^1J_{CH_{ax}}$. These results are compatible with the conclusion that the main factor defining the experimental difference between $^1J_{CH_{ax}}$ and $^1J_{CH_{eq}}$ SSCCs is the negative hyperconjugative interaction $n(O) \rightarrow \sigma^*_{CH_{ax}}$.

E. Geometric Effect on $^1J_{CH}$ SSCCs. Results displayed in Table 6 show that in methane, where hyperconjugative interactions are very small, how $^1J_{CH_a}$ SSCC is affected by a distortion in the molecular geometry. That distortion was obtained increasing the H_a-C-H bond angles from tetrahedral to 120°, keeping the $C-H_a$ direction as a 3-fold symmetry axis. It is also observed an important increase in the s % character at the C atom of the σ_{CH_a} bond. This geometry effect on a $^1J_{CH}$ SSCC is expected to be present when other effects are also operating, like, for instance, hyperconjugative and/or electrostatic interactions. Of course, in actual compounds all these effects are strongly intertwined, and it might be impossible to obtain a neat separation between them. However, in some instances indirect evidence might be obtained on any of these effects; this seems to be the case of $^1J_{C_2H}$ in compounds **Ib** where such couplings were measured as part of this work (Table 1), and their total calculated values are shown in Table 2. In fact, it is observed that, although small, there is a systematic difference between such couplings in series **Ia** and **Ib** (Table 10), which is rather insensitive to the nature of the X substituent. In Table 10 are collected also the difference in the bridgehead C_1- - -C_3 distance, $\Delta(d_{C_1C_3})$, obtained from their optimized geometries and between the C_2 s % character, Δ(s %), as given by the NBO method between compounds of series **Ia** and **Ib** for the same X substituent. It is observed that the methyl group, series **Ib**, yields an increase in $d_{C_1C_3}$ of about (8 to 10) × 10^{-3} Å, which also decreases the C_2 s % character in ca. 0.4% for the σ_{C_2H} bond. On the other hand, a qualitative analysis of how hyperconjugative interactions affect the respective J^b and J^{ob} contributions to the FC term of such couplings show that these effects tend to compensate among each other (Table 11). These observations are compatible with ascribing to a geometric effect (i.e. a slight lengthening of the bridgehead C_1- - -C_3 distance), the changes

TABLE 11: Occupancies (given as in Table 3) of Bonds and Antibonds Relevant for a Qualitative Analysis of J^b and J^{ob} to the FC Term of $^1J_{C_2H}$ SSCCs in Ia and Ib

	σ_{C_2H}		$\sigma^*_{C_2H}$		$\sigma_{C_1C_2}$		$\sigma_{C_2C_3}$	
X	**Ia**	**Ib**	**Ia**	**Ib**	**Ia**	**Ib**	**Ia**	**Ib**
H	−9	−10	19	19	−37	−40	−37	−46
CH_2OH	−10	−10	18	19	−48	−50	−40	−50
$COCH_3$	−9	−10	19	19	−53	−57	−40	−50
$CONH_2$	−9	−10	19	19	−53	−56	−40	−50
CO_2H	−9	−10	18	18	−52	−56	−40	−50
CN	−9	−10	18	18	−58	−61	−40	−50
NH_2	−10	−11	19	20	−43	−48	−43	−53
NO_2	−10	−11	17	17	−49	−52	−50	−59
Cl	−10	−11	18	18	−38	−41	−56	−65
Br	−10	−11	18	18	−38	−41	−57	−67
I	−10	−11	18	18	−37	−41	−58	−68

observed in $^1J_{C_2H}$ SSCCs when comparing analogous compounds in series **Ib** and **Ia**.

5. Concluding Remarks

In the qualitative analysis of how hyperconjugative interactions affect $^1J_{C(sp)^3,H}$ SSCCs presented in Section 2, it is concluded that (a) hyperconjugative interactions whether from the σ_{CH} bond or to the σ^*_{CH} antibond (both of them involving the coupling nuclei) yield a reduction on the $^1J_{C(sp)^3,H}$ SSCC; (b) hyperconjugative interactions from any of the three "other bonds" involving the coupling C nucleus yield an increase in that $^1J_{C(sp)^3,H}$ SSCC. Experimental $^1J_{C_3H}$ couplings measured in members of the **Ia** series support conclusion (b).

Effects of changes in the polarization along the σ_{CH} bond on the corresponding $^1J_{C(sp)^3,H}$ SSCC are studied resorting to model systems **II** and **III**. Such results show that polarization of the σ_{CH} bond by an electric field along that bond and pointing in this way, C → H, yields an increase on the corresponding $^1J_{C(sp)^3,H}$ SSCC. This result is compatible with experimental values taken from the current bibliography. Conspicuous examples are those observed in weak hydrogen bonds of type C−H- - -O, now recognized as very important in biological compounds. A reversal of the polarization along that bond yields a reduction of such a coupling.

In many instances electrostatic interactions, like for instance, in models **IIIa** and **IIIb**, are notably intertwined with hyperconjugative interactions. In fact, the latter can be inhibited (enhanced) by electrostatic interactions depending on the orientation of the electric field. Despite such sensitivity of hyperconjugative interactions on electrostatic effects, results shown for models **IVa** and **IVb** suggest that the main effect defining the difference between $^1J_{C_1H_{eq}}$ and $^1J_{C_1H_{ax}}$ in **IV** originates mainly in the strong negative hyperconjugative interaction affecting the $\sigma_{CH_{ax}}$ bond (i.e., $n(O) \rightarrow \sigma^*_{CH_{ax}}$).

Acknowledgment. The following financial supports are gratefully acknowledged; CONICET (Grant 2140/99) and UBACyT (Grant X222) (Argentina); FAPESP (Grant 02/12305-6) for a fellowship (C.F.T.) and CNPq for a scholarship (F.P.S.) (Brazil); Dirección General de Enseñanza Superior e Investigación Científica (Grant BQU2000-0211-CO2) (Spain); and Australian Research Council (E.W.D. and I.J.L., Australia).

References and Notes

(1) Eliel, E. L. 100+ years of conformational analysis. In *Conformational Behavior, and Six-Membered Rings: Analysis, Dynamics, and Stereoelectronic Effects*; Juaristi, E. Ed.; VCH Publishers: New York, 1995.

(2) Dewar, M. J. S.; Dougherty, R. C. *The PMO Theory of Organic Chemistry*; Plenum Press: New York, 1975.

(3) (a) Reed, A. E.; Curtiss, L. A.; Weinhold, F. *Chem. Rev.* **1988**, *88*, 899−926. (b) Weinhold F. In *Encyclopedia of Computational Chemistry*; Schleyer, P. v. R., Ed.; Wiley: New York, 1998; Vol. 3, p 1792.

(4) (a) Edison, A. S.; Markley, J. L.; Weinhold, F. *J. Biomol NMR* **1995**, *5*, 332−332. (b) Esteban, A. L.; Galache, M. P.; Mora, F.; Díez, E.; Casanueva, E. J.; San Fabián, J.; Barone V.; Peralta, J. E.; Contreras, R. H. *J. Phys. Chem*. A **2001**, *105*, 5298−5303.

(5) (a) Contreras, R. H.; Facelli, J. C. *Annu. Rep. NMR Spectrosc.* **1993**, *27*, 255−356. (b) Contreras, R. H.; Peralta, J. E.; Giribet, C. G.; Ruiz de Azúa, M. C.; Facelli, J. C. *Annu. Rep. NMR Spectrosc.* **2000**, *41*, 55−184. (c) Contreras, R. H.; Peralta, J. E. *Prog. NMR Spectrosc.* **2000**, *37*, 321−425. (d) Contreras, R. H.; Barone, V.; Peralta, J. E.; Facelli, J. C. *Annu. Rep. NMR Spectrosc.* **2000**, *51*, 167−260. (e) Tormena, C. F.; Rittner, R.; Contreras, R. H.; Peralta, J. E. *J. Phys. Chem. A* **2004**, *108*, 7762−7768.

(6) (a) Kirby, A. J. *The Anomeric Effect and Related Stereoelectronic Effects at Oxygen*; Springer-Verlag: Berlin, 1983. (b) Juaristi, E.; Cuevas, G. *The Anomeric Effect*; CRC Press: Boca Raton, FL, 1994. (c) Juaristi, E., Ed. *Conformational Behavior of Six-Membered Rings: Analysis, Dynamics, and Stereoelectronic Effects*; VCH Publishers: New York, 1995. (d) Uehara, F.; Sato, M.; Kaneko, C.; Kurihara, H. *J. Org. Chem.* **1999**, *64*, 1436−1441. (e) Alabugin, I. V. *J. Org. Chem.* **2000**, *65*, 3910−3919. (f) Perrin, C. L. *Acc. Chem. Res.* **2002**, *35*, 28−34.

(7) Reed, A. E.; Schleyer, P. v. R. *J. Am. Chem. Soc.* **1990**, *112*, 1434−1445.

(8) (a) Hoffman, R. A. *Mol. Phys.* **1958**, *1*, 326−330. (b) Barfield, M.; Chakrabarti, B. *Chem. Rev.* **1969**, *69*, 757−778.

(9) Contreras, R. H.; Esteban, A. L.; Díez, E., Head, N. J.; Della, E. W. *Mol. Phys*. **2006**, *104*, 485−492.

(10) (a) Cuevas, G.; Juaristi, E. *J. Am. Chem. Soc*. **2002**, *124*, 13088−13096. (b) Mayorga, K. M.; Juaristi, E.; Cuevas, G. *J. Org. Chem*. **2004**, *69*, 7266−7276.

(11) (a) Gil, M. S.; von Philipsborn, W. *Magn. Reson. Chem.* **1989**, *27*, 409−430. (b) Krivdin, L. B.; Kalabin, G. A. *Prog. NMR Spectrosc.* **1989**, *21*, 293−448. (c) Kamienska-Trela, K. *Annu. Rep. NMR Spectrosc*. **1995**, *30*, 131−229.

(12) Cuevas, G.; Martínez-Mayorga, K.; Fernández-Alonso, M. C.; Jiménez-Barbero, J.; Perrin, C. L.; Juaristi, E.; López-Mora, N. *Angew. Chem., Int. Ed.* **2005**, *44*, 2360−2364.

(13) (a) Perlin, A. S.; Casu, B. *Tetrahedron Lett.* **1969**, *10*, 2921−2924. (b) Wolfe, S.; Pinto, B. M.; Varma, V.; Leung, R. Y. N. *Can. J. Chem.* **1990**, *68*, 1051−1062.

(14) (a) Afonin, A. V.; Andryankov, M. A. *Zh. Org. Khim*. **1988**, *24*, 1034. (b) Afonin, A. V.; Sigalov, M. V.; Korustova, S. E.; Aliev, I. A.; Vashchenko, A. V.; Trofimov, B. A. *Magn. Reson. Chem.* **1990**, *28*, 580. (c) Satonaka, H.; Abe, K.; Hirota, M. *Bull. Chem. Soc. Jpn*. **1988**, *61*, 2031. (d) Mele, A.; Vergani, B.; Viani, F.; Meille, S. V.; Farina, A.; Bravo, P. *Eur. J. Org. Chem.* **1999**, 187. (e) Biekofsky, R. R.; Pomilio, A. B.; Contreras, R. H. *J. Mol. Struct. Theochem*. **1990**, *210*, 211−219. (f) Vizioli, C. V.; Ruiz de Azúa, M. C.; Giribet, C. G.; Contreras, R. H.; Turi, L.; Dannenberg, J. J.; Rae, I. D.; Weigold, J. A.; Malagoli, M.; Zanasi, R.; Lazzeretti, P. *J. Phys. Chem*. **1994**, *98*, 8858−8861. (g) Giribet, C. G.; Vizioli, C. V.; Ruiz de Azúa, M. C.; Contreras, R. H.; Dannenberg, J. J.; Masunov, A. *J. Chem. Soc., Faraday Trans*. **1996**, *92*, 3029−3033. (h) de Kowalewski, D. G.; Kowalewski, V. J.; Peralta, J. E.; Eskuche, G.; Contreras, R. H.; Esteban, A. L.; Galache, M. P.; Díez, E. *Magn. Reson. Chem*. **1999**, *37*, 227−231.

(15) (a) Adcock, W.; Krstic, A. R. *Tetrahedron Lett.* **1992**, *33*, 7397−7398. (b) Matta, C. F.; Hernández-Trujillo, J.; Bader, R. F. W. *J. Phys. Chem. A* **2002**, *106*, 7369−7375.

(16) Della, E. W.; Lochert, I. J.; Peralta J. E.; Contreras, R. H. *Magn. Reson. Chem.* **2000**, *38*, 395−402.

(17) Contreras, R. H.; Esteban, A. L.; Díez, E.; Della, E. W.; Lochert, I. J. *Magn. Reson. Chem.* **2004**, *42*, S202−S206.

(18) Della, E. W.; Lochert, I. J.; Peruchena, N. M.; Aucar G. A.; Contreras, R. H. *J. Phys. Org. Chem.* **1996**, *9*, 168−178.

(19) Barone, V.; Peralta, J. E.; Contreras, R. H. *J. Comput. Chem*. **2001**, *22*, 1615−1621.

(20) Sychrovský, V.; Gräfenstein, J.; Cremer, D. *J. Chem. Phys*. **2000**, *113*, 3530−3547.

(21) Frisch, M. J.; Trucks, G. W.; Schlegel, H. B.; Scuseria, G. E.; Robb, M. A.; Cheeseman, J. R.; Montgomery, J. A., Jr.; Vreven, T.; Kudin, K. N.; Burant, J. C.; Millam, J. M.; Iyengar, S. S.; Tomasi, J.; Barone, V.; Mennucci, B.; Cossi, M.; Scalmani, G.; Rega, N.; Petersson, G. A.; Nakatsuji, H.; Hada, M.; Ehara, M.; Toyota, K.; Fukuda, R.; Hasegawa, J.; Ishida, M.; Nakajima, T.; Honda, Y.; Kitao, O.; Nakai, H.; Klene, M.; Li, X.; Knox, J. E.; Hratchian, H. P.; Cross, J. B.; Bakken, V.; Adamo, C.; Jaramillo, J.; Gomperts, R.; Stratmann, R. E.; Yazyev, O.; Austin, A. J.; Cammi, R.; Pomelli, C.; Ochterski, J. W.; Ayala, P. Y.; Morokuma, K.; Voth, G. A.; Salvador, P.; Dannenberg, J. J.; Zakrzewski, V. G.; Dapprich, S.; Daniels, A. D.; Strain, M. C.; Farkas, O.; Malick, D. K.; Rabuck, A. D.; Raghavachari, K.; Foresman, J. B.; Ortiz, J. V.; Cui, Q.; Baboul, A.

G.; Clifford, S.; Cioslowski, J.; Stefanov, B. B.; Liu, G.; Liashenko, A.; Piskorz, P.; Komaromi, I.; Martin, R. L.; Fox, D. J.; Keith, T.; Al-Laham, M. A.; Peng, C. Y.; Nanayakkara, A.; Challacombe, M.; Gill, P. M. W.; Johnson, B.; Chen, W.; Wong, M. W.; Gonzalez, C.; Pople, J. A. *Gaussian 03*, revision B.01; Gaussian, Inc.: Wallingford, CT, 2004.

(22) Glendening E. D.; Reed, A. E.; Carpenter, J. E.; Weinhold, F. *NBO version 3.1*; Program as implemented in the *Gaussian 03* package.

(23) (a) Oddershede, J. *Adv. Quantum Chem.* (b) Diz, A. C.; Giribet C. G.; Ruiz de Azúa, M. C.; Contreras, R. H. *Int. J. Quantum Chem*. **1990**, *37*, 663−677. (c) Contreras, R. H.; Ruiz de Azúa, M. C.; Giribet, C. G.; Aucar, G. A.; Lobayan de Bonczok, R. *J. Mol. Struct. Theochem* **1993**, *284*, 249−269. (d) Giribet, C. G.; Ruiz de Azúa, M. C.; Contreras, R. H.; Lobayan de Bonczok, R.; Aucar, G. A.; Gomez, S. *J. Mol. Struct. Theochem.* **1993**, *300*, 467−477.

(24) Lochert, I.J. Ph.D. Thesis, Flinders University, 1996.

(25) Lee, C.; Yang, W.; Parr, R. G. *Phys. Rev.* B **1988**, *37*, 785−789.

(26) (a) Becke, A. D. *Phys. Rev. A* **1988**, *38*, 3098−3100. (b) Becke, A. D. *J. Chem. Phys*. **1993**, *98*, 5648−5652.

(27) Barone, V. *J. Chem. Phys.* **1994**, *101*, 6834−6838.

(28) Peralta, J. E.; Scuseria, G. E.; Cheeseman, J. R.; Frisch, M. J. *Chem. Phys. Lett.* **2003**, *375*, 452−458.

(29) (a) Lutnæs, O. B.; Ruden, T. A.; Helgaker, T. *Magn. Reson. Chem*., **2004**, *42*, S117−S127. (b) Wigglesworth, R. D.; Raynes, W. T.; Kirpekar, S.; Oddershede, J.; Sauer, S. P. A. *J. Chem. Phys*. **2000**, *112*, 3735−3746.